

Landau Quantization of Topological Surface States in Bi₂Se₃

Peng Cheng,¹ Canli Song,¹ Tong Zhang,^{1,2} Yanyi Zhang,¹ Yilin Wang,² Jin-Feng Jia,¹ Jing Wang,¹ Yayu Wang,¹
 Bang-Fen Zhu,¹ Xi Chen,^{1,*} Xucun Ma,^{2,†} Ke He,² Lili Wang,² Xi Dai,² Zhong Fang,² Xincheng Xie,² Xiao-Liang Qi,^{3,4}
 Chao-Xing Liu,^{4,5} Shou-Cheng Zhang,⁴ and Qi-Kun Xue^{1,2}

¹*Department of Physics, Tsinghua University, Beijing 100084, China*

²*Institute of Physics, Chinese Academy of Sciences, Beijing 100190, China*

³*Microsoft Research, Station Q, University of California, Santa Barbara, California 93106, USA*

⁴*Department of Physics, Stanford University, Stanford California 94305, USA*

⁵*Physikalisches Institut, Universität Würzburg, D-97074 Würzburg, Germany*

(Received 25 May 2010; published 9 August 2010)

We report the direct observation of Landau quantization in Bi₂Se₃ thin films by using a low-temperature scanning tunneling microscope. In particular, we discovered the zeroth Landau level, which is predicted to give rise to the half-quantized Hall effect for the topological surface states. The existence of the discrete Landau levels (LLs) and the suppression of LLs by surface impurities strongly support the 2D nature of the topological states. These observations may eventually lead to the realization of quantum Hall effect in topological insulators.

DOI: 10.1103/PhysRevLett.105.076801

PACS numbers: 73.20.-r, 68.37.Ef, 71.70.Di, 72.25.Dc

The recent theoretical prediction and experimental realization [1–14] of topological insulators (TI) have generated intense interest in this new state of quantum matter. The surface states of a three-dimensional (3D) TI such as Bi₂Se₃ [12], Bi₂Te₃ [13], and Sb₂Te₃ [14] consist of a single massless Dirac cone [9]. Crossing of the two surface state branches with opposite spins in the materials is fully protected by the time-reversal (TR) symmetry at the Dirac points, which cannot be destroyed by any TR invariant perturbation. Recent advances in thin-film growth [15,16] have permitted this unique two-dimensional electron system (2DES) to be probed by scanning tunneling microscopy (STM) and spectroscopy (STS) [17]. The intriguing TR symmetry protected topological states were revealed in STM experiments where the backscattering induced by nonmagnetic impurities is forbidden [17–19]. Here we report the Landau quantization of the topological surface states in Bi₂Se₃ in magnetic field by using STM and STS. The direct observation of the discrete Landau levels (LLs) and the suppression of LLs by surface impurities strongly support the 2D nature of the topological states. Furthermore, the dependence of LLs on magnetic field is demonstrated to be consistent with the cone structure of the surface states. The formation of LLs also implies the high mobility of the 2DES, which has been predicted to lead to topological magnetoelectric effect of the TI [7,20].

The experiments were conducted at 4.2 K in a Unisoku ultrahigh vacuum low-temperature STM system equipped with molecular beam epitaxy (MBE) for film growth. As shown in previous works [15,16], the MBE films of TI have lower carrier density than those prepared by the self-flux technique. We epitaxially grew the single crystalline Bi₂Se₃ films on graphitized 6H-SiC(0001) substrate, which is nitrogen doped (*n* type) with a resistivity of

0.03 Ω/cm and thickness of 0.1 mm. The graphene was grown on SiC by thermal desorption of silicon at 1300 °C after the sample had been heated to 850 °C in Si flux for several cycles to form Si-rich 3 × 3 reconstruction. High purity Bi (99.999%) and Se (99.999%) were thermally evaporated from Knudsen cells. The temperatures of the Bi source, the Se source, and the substrate are 455, 170, and 230 °C, respectively. Figure 1(a) shows a typical STM image of the atomically flat Bi₂Se₃ film with a thickness of 50 quintuple layers (QL) grown by MBE. The steps on the surface are preferentially oriented along the close-packing directions and have the height (0.95 nm) of a quintuple layer. The atomically resolved STM image [Fig. 1(b)] exhibits the hexagonal lattice structure of the Se-terminated (111) surface of Bi₂Se₃ [21–23]. The STM images reveal a very small density of defects (approximately 1 per 50 nm²) on the surface. Most of the defects [Fig. 1(c)] are either clover-shaped protrusions [21–23] or triangular depressions, which can be assigned to the substitutional Bi defects at Se sites or the Se vacancies, respectively.

In STS, the differential tunneling conductance dI/dV measures the local density of states (LDOS) of electrons at energy eV , where $-e$ is the charge on an electron. Figure 1(d) shows the dI/dV spectrum on the Bi₂Se₃ surface at zero magnetic field. The Dirac point of the topological states corresponds to the minimum (indicated by an arrow) of the spectrum and is about 200 meV below the Fermi level. However, the Fermi level determined by angle-resolved photoemission spectroscopy (ARPES) [16] on 50 QL film is only 120 meV above the Dirac point [24]. The discrepancy is due to the electrostatic induction by the electric field between the STM tip and sample, which has been observed in 2D systems with low electron

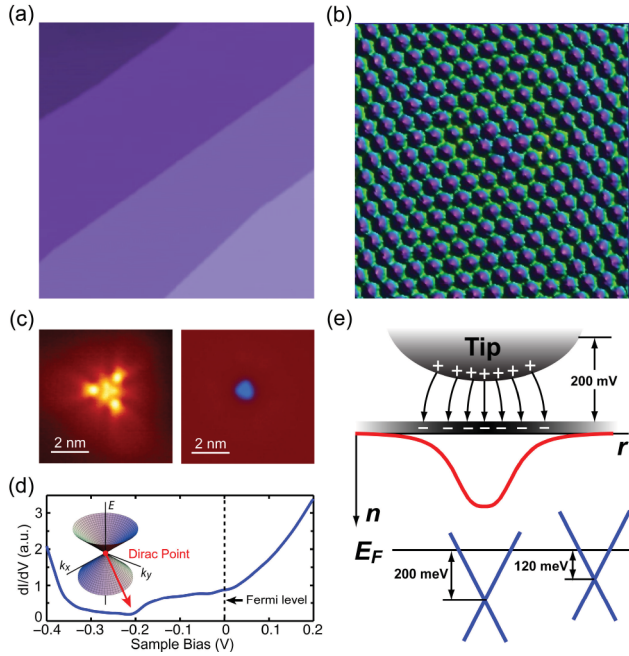


FIG. 1 (color). Bi_2Se_3 film prepared by MBE. (a) The STM image ($200 \text{ nm} \times 200 \text{ nm}$) of the $\text{Bi}_2\text{Se}_3(111)$ film. Imaging conditions: $V = 4.0 \text{ V}$, $I = 0.1 \text{ nA}$. The bias voltage is applied to the sample. (b) The atomic-resolution image of the $\text{Bi}_2\text{Se}_3(111)$ surface (1 mV , 0.2 nA). Each spot in the image corresponds to a Se atom. Selenium atom spacing is about 4.14 \AA . (c) The defects on the surface of Bi_2Se_3 . The left and the right images (both taken at -0.3 V , 0.1 nA) show the substitutional Bi defect and the Se vacancy, respectively. (d) dI/dV spectrum taken on the $\text{Bi}_2\text{Se}_3(111)$ surface. Set point: $V = 0.2 \text{ V}$, $I = 0.12 \text{ nA}$. The Dirac point is indicated by an arrow. The single Dirac cone band structure of Bi_2Se_3 is schematically shown in the inset. (e) The energy band shifts appreciably in the presence of STM tip. The red curve depicts the electron density n as a function of the lateral distance r from the apex of tip.

density [25]. The MBE film of Bi_2Se_3 with high quality is a bulk insulator. The surface states of the film are fully responsible for screening and susceptible to external electric field due to the low density of states. The density of the induced charges on the surface in the presence of a tip is roughly given by $\epsilon_0 V/d$, where V and d are the sample bias voltage and the distance between tip and sample, respectively. With $V \sim 100 \text{ mV}$ and $d \sim 1 \text{ nm}$, the induced density of electrons is typically in the order of 10^{12} cm^{-2} , which is comparable to the intrinsic carrier density on the surface without a tip. With negative bias voltage as shown in Fig. 1(e), the field effect moves the Dirac cone (and also the Dirac point) downwards to accommodate the induced charges, leading to a bias-dependent Dirac point.

If the electrostatic effect is negligible, a quantum state can be accessed by STM at bias voltage $V = E/e$, where E is the energy of the state with respect to the Fermi level. However, in the case of Bi_2Se_3 , eV and the energy E of a

state on the Dirac cone without a tip are considerably different. To take into account the electrostatic effect, we consider the simplest approximation which models the tunneling junction as a parallel plate capacitor. Knowing the energies of the Dirac points with ($E_D = -200 \text{ meV}$) and without ($E_D^0 = -120 \text{ meV}$) a tip, a straightforward calculation leads to

$$E = eV + E_D^0 \left[1 - \sqrt{1 + \left(\frac{E_D}{E_D^0} - \frac{E_D^0}{E_D} \right) \frac{eV}{E_D^0}} \right]. \quad (1)$$

The calibration by the above equation is needed to reliably interpret the STM data on topological insulators.

When magnetic field is applied to a 2DES, the energy spectrum of the system is quantized into LLs as shown in previous experiments on various 2DESs [25–30]. For topological insulators, the high quality of the MBE films ensures the observation of LLs. The magnetic field dependence of tunneling conductance in Fig. 2 clearly reveals the development of well-defined LLs (the series of peaks) in Bi_2Se_3 with increasing field. The spectra demonstrate a direct measurement of the Landau quantization of the topological surface states. Under strong magnetic field, more than ten unequally spaced LLs are explicitly resolved above the Dirac point (for example, see the black curve for a magnetic field of 11 T in Fig. 2). Very likely, the absence of LLs below the Dirac point results from the overlapping of the surface states with the bulk valence band [12].

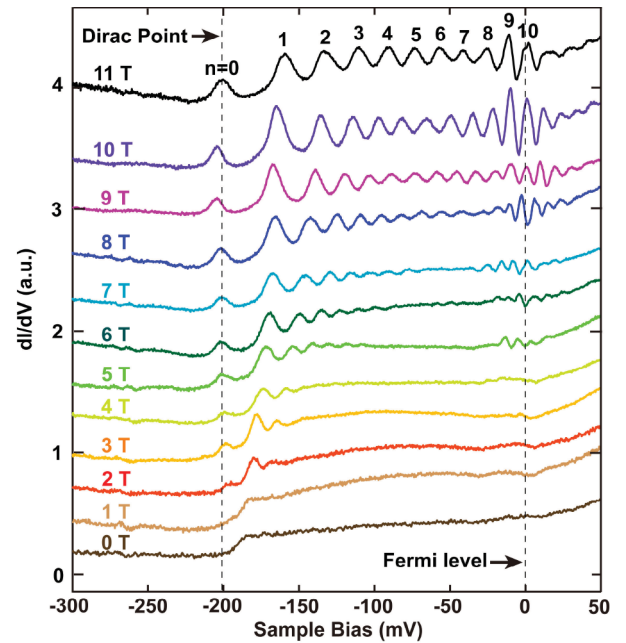


FIG. 2 (color). Landau quantization of the topological states. The film is 50 QL thick. The differential tunneling spectra were acquired for various magnetic fields from 0 to 11 T . The field is perpendicular to the surface. The set point of STS is 0.1 V and 0.12 nA . The bias modulation was 2 mV (rms) at 913 Hz . The curves are offset vertically for clarity.

We further confirm the 2D nature of the quantized states by evaporating Ag atoms onto the surface of Bi_2Se_3 [Fig. 3]. Presumably, the LLs are sensitive to the defect scattering if the impurities are located within the 2DES. Compared with the undoped samples, the Dirac point shifts downwards in energy because of the electron transfer from the Ag atoms to the substrate. At low defect density [Fig. 3(a)], no explicit change in the tunneling spectrum has been observed. The defect scattering comes into effect [Fig. 3(b)] when the distance between impurities in the 2DES is comparable to the magnetic length $l_B \sim \sqrt{\hbar/eB} \sim 10$ nm at 11 T, where \hbar is Planck's constant h divided by 2π . Finally, at even higher Ag atom coverage [Fig. 3(c)], the Landau quantization is completely suppressed as expected. The presence of distinct peaks and the suppression of LLs by surface impurities strongly indicate that the peaks in Fig. 2 is due to Landau quantization of the topological surface states within the bulk gap of Bi_2Se_3 .

The Landau quantization of the topological states of Bi_2Se_3 has some common features with that of graphene [27–29]. Unlike the Landau levels of a 2DES with parabolic dispersion, the peaks in the spectra in Fig. 2 are not equally spaced. In addition, there is always one peak residing at the Dirac point (-200 mV) in each dI/dV

spectrum. The energy of such LL is independent of the magnetic field [31]. In the lowest order approximation, the topological surface states of Bi_2Se_3 can be modeled by the massless Dirac equation. Unique to the massless Dirac fermions, the energy of the n th level LL_n has a square-root dependence on magnetic field B :

$$E_n = E_D^0 + \text{sgn}(n)v_F\sqrt{2eB\hbar|n|}, \quad n = 0, \pm 1, \pm 2, \dots, \quad (2)$$

where v_F is the Fermi velocity. Here we neglect the effect of the Zeeman splitting which only leads to a correction of about 1 meV to the Landau level spectrum for the magnetic field range ($B \leq 11$ T) we used. The number of electrons per unit area on a Landau level is proportional to the magnetic field and given by $n_L = eB/2\pi\hbar$. Notably, the Dirac fermion model shows that the energy of LL_0 is independent of B . We therefore identify the peaks at the Dirac point (indicated by the vertical dotted line at -200 mV in Fig. 2) as LL_0 . As predicted by the field theory of topological insulators, the existence of such zero-mode level is crucial for the topological magnetoelectric effect defining the TI [7,20]. Leaving the $n = 0$ level empty or completely filling it gives rise to the quantum Hall effect with Hall conductance $-1/2$ or $+1/2$ in units of e^2/h .

The Dirac fermion nature of the electrons is further revealed by plotting the energy of LLs, which has been calibrated by Eq. (1), versus \sqrt{nB} [Fig. 4]. The peak positions of LLs are determined by fitting the differential conductance in Fig. 2 with multiple Gaussians. In Fig. 4, all the data collapse to a single line, suggesting that the energy of LLs is scaled as \sqrt{nB} . Fitting the data to a

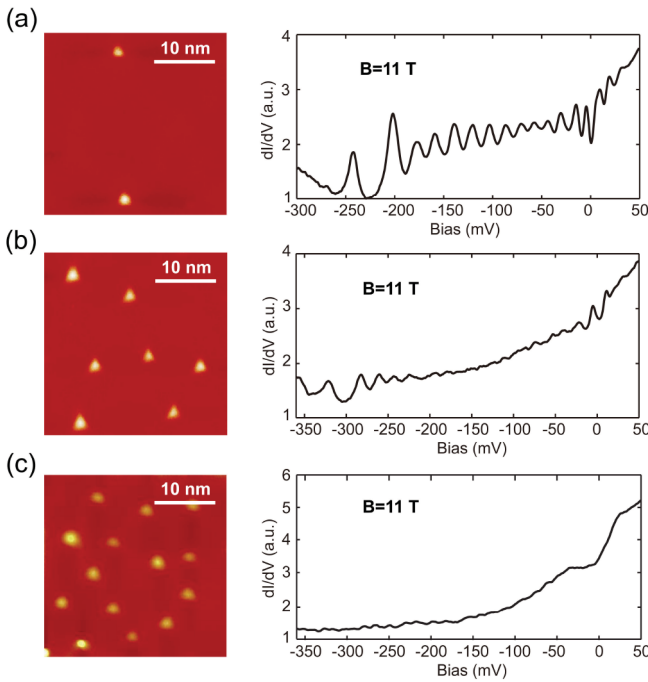


FIG. 3 (color). Suppression of LLs by defects. The three panels show the STM images and the corresponding STS spectra of LLs at different Ag impurity densities, respectively. An individual Ag atom is imaged as a triangular spot. The imaging conditions are 0.5 V and 0.04 nA. The LLs do not change at low density of impurities (0.0002 ML coverage) (a), but are partially suppressed (b) as the average distance between Ag impurities becomes ~ 10 nm (0.0006 ML coverage). (c) The LLs are fully suppressed at even higher impurity coverage.

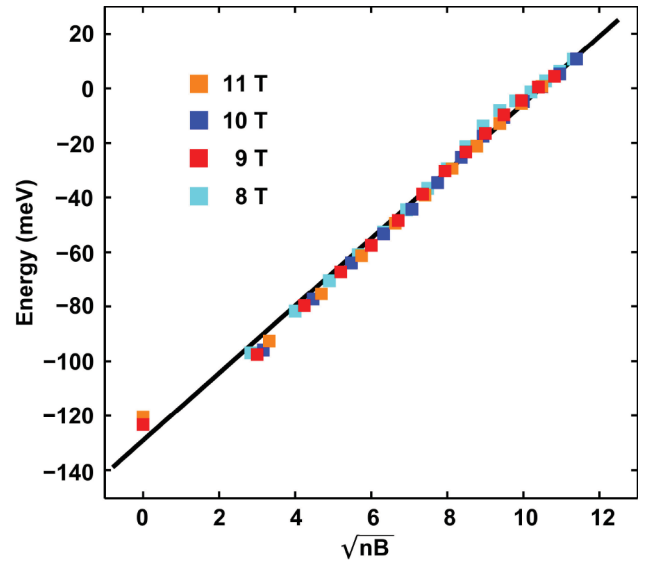


FIG. 4 (color). The fitting to the LL energies for magnetic fields from 8 to 11 T. Different colors correspond to the LL energies at different magnetic field.

straight line gives $v_F = 3.4 \times 10^5$ m/s, which is compared to 5×10^5 m/s by ARPES measurement [12]. The difference is probably due to the nonlinearity of the band dispersion. The value of v_F depends on the position of the Fermi level, which varies in the samples prepared by different methods [12,16].

The observation of Landau quantization may eventually lead to the realization of quantum Hall effect in topological insulators. Further efforts are required to design a feasible procedure to fabricate the multiterminal devices based on topological insulators for transport measurements. The STM topographic images were processed using WSXM [32].

The work is supported by NSFC and the National Basic Research Program of China.

Note added.—Recently, we became aware of related work by T. Hanaguri *et al.* [33].

*xc@mail.tsinghua.edu.cn

†xcma@aphy.iphy.ac.cn

- [1] X.-L. Qi and S.-C. Zhang, *Phys. Today* **63**, No. 1, 33 (2010).
- [2] J. E. Moore, *Nature (London)* **464**, 194 (2010).
- [3] M. Z. Hasan and C. L. Kane, [arXiv:1002.389](https://arxiv.org/abs/1002.389).
- [4] L. Fu, C. L. Kane, and E. J. Mele, *Phys. Rev. Lett.* **98**, 106803 (2007).
- [5] L. Fu and C. L. Kane, *Phys. Rev. B* **76**, 045302 (2007).
- [6] J. E. Moore and L. Balents, *Phys. Rev. B* **75**, 121306 (2007).
- [7] X.-L. Qi, T. L. Hughes, and S.-C. Zhang, *Phys. Rev. B* **78**, 195424 (2008).
- [8] R. Roy, *Phys. Rev. B* **79**, 195321 (2009).
- [9] H. J. Zhang *et al.*, *Nature Phys.* **5**, 438 (2009).
- [10] M. König *et al.*, *Science* **318**, 766 (2007).
- [11] D. Hsieh *et al.*, *Nature (London)* **452**, 970 (2008).
- [12] Y. Xia *et al.*, *Nature Phys.* **5**, 398 (2009).
- [13] Y. L. Chen *et al.*, *Science* **325**, 178 (2009).
- [14] D. Hsieh *et al.*, *Phys. Rev. Lett.* **103**, 146401 (2009).
- [15] Y. Y. Li *et al.*, *Adv. Mater.* (to be published).
- [16] Y. Zhang *et al.*, *Nature Phys.* **6**, 584 (2010).
- [17] T. Zhang *et al.*, *Phys. Rev. Lett.* **103**, 266803 (2009).
- [18] P. Roushan *et al.*, *Nature (London)* **460**, 1106 (2009).
- [19] Z. Alpichshev *et al.*, *Phys. Rev. Lett.* **104**, 016401 (2010).
- [20] X.-L. Qi, R. D. Li, J. D. Zang, and S.-C. Zhang, *Science* **323**, 1184 (2009).
- [21] Y. S. Hor *et al.*, *Phys. Rev. B* **79**, 195208 (2009).
- [22] S. Urzhidin *et al.*, *Phys. Rev. B* **66**, 161306 (2002).
- [23] S. Urzhidin *et al.*, *Phys. Rev. B* **69**, 085313 (2004).
- [24] For comparison, the Dirac point of bulk crystal is 0.3 eV below the Fermi level due to the higher carrier density.
- [25] M. Morgenstern *et al.*, *J. Electron Spectrosc. Relat. Phenom.* **109**, 127 (2000).
- [26] T. Matsui *et al.*, *Phys. Rev. Lett.* **94**, 226403 (2005).
- [27] G. H. Li and E. Y. Andrei, *Nature Phys.* **3**, 623 (2007).
- [28] G. H. Li, A. Luican, and E. Y. Andrei, *Phys. Rev. Lett.* **102**, 176804 (2009).
- [29] D. L. Miller *et al.*, *Science* **324**, 924 (2009).
- [30] S. Becker, M. Liebmann, T. Mashoff, M. Pratzner, and M. Morgenstern, *Phys. Rev. B* **81**, 155308 (2010).
- [31] The energies of these $n = 0$ peaks slightly shift with magnetic field as a result of the redistribution of electron density of states due to the formation of LLs.
- [32] www.nanotec.es
- [33] T. Hanaguri, K. Igarashi, M. Kawamura, H. Takagi, and T. Sasagawa, [arXiv:1003.0100](https://arxiv.org/abs/1003.0100) [*Phys. Rev. B* (to be published)].